

## EXPERIMENTS ON MELT DISPERSION WITH LATERAL FAILURE IN THE BOTTOM HEAD OF THE PRESSURE VESSEL

*L. MEYER, M. GARGALLO*

Forschungszentrum Karlsruhe, Institut für Kern-und Energietechnik, Postfach 3640  
76021 Karlsruhe, Germany, e-mail: meyer@iket.fzk.de

KEYWORDS: Severe accident, Vessel failure, Two-phase flow

### **Abstract**

Melt dispersion experiments with lateral failure in the bottom head were carried out in a 1:18 scaled annular cavity design under low pressure conditions. Water and a bismut-alloy were used as melt simulant material and nitrogen as driving gas. With lateral breaches the liquid height in the lower head relative to the upper and lower edge of the breach is an additional parameter for the dispersion process. Shifting the break from the central position towards the side of the lower head leads to smaller melt dispersion, and a larger breach size does not necessarily lead to a larger dispersed melt fraction.

### **Introduction**

In a severe accident with melting of the core special pressure relief valves in the primary circuit of German Pressurized Water Reactors (PWR) and future European Reactors will reduce the system pressure below 20 bar. A failure in the bottom head of the reactor pressure vessel, followed by melt expulsion and blowdown of the reactor cooling system, might disperse molten core debris out of the reactor pit, even at low pressures. The mechanisms of efficient debris-to-gas heat transfer, exothermic metal/oxygen reactions, and hydrogen combustion may cause a rapid increase in pressure and temperature in the reactor containment and are collectively referred to as Direct Containment Heating (DCH). A number of problems have to be addressed: (1) final location of corium debris, (2) loads on the containment in respect to pressure and temperature, (3) amount of hydrogen produced, (4) loads on reactor pit and support structures, (5) impact on safety components.

A large amount of work has been done, mainly in the USA, to investigate the melt dispersal/DCH-phenomena for cavity designs with large instrument tunnels leading into subcompartments [1]. Only few experiments have been done with an annular cavity design [2-5]. Some European PWRs and the planned European Pressurized Reactor (EPR) have an annular cavity design where the only large pathway out of the cavity is the narrow annular gap between the reactor pressure vessel (RPV) and the cavity wall. The past experiments focused on relatively small holes at the center of the lower head and high failure pressures. Our investigations have been extended to

low failure pressures and larger breach sizes in an annular cavity design, and lateral breaches were investigated for the first time.

A test facility has been built at Forschungszentrum Karlsruhe for performing dispersion experiments with cold simulant materials in a 1/18 scale. The fluids were water or bismuth alloy instead of melt, and nitrogen or helium instead of steam. Experiments with different materials are necessary to validate scaling laws. The first series of experiments with central holes in the lower head showed large dispersal of the liquids (up to 76%) into the pump and steam generator rooms with pressures as low as 6 bar. These results have been published already [6,7]. In the second part of the experimental program a detailed investigation of geometry effects was performed, such as lateral holes, lateral slots, and unzipping of the lower head. The results of these experiments are presented here.

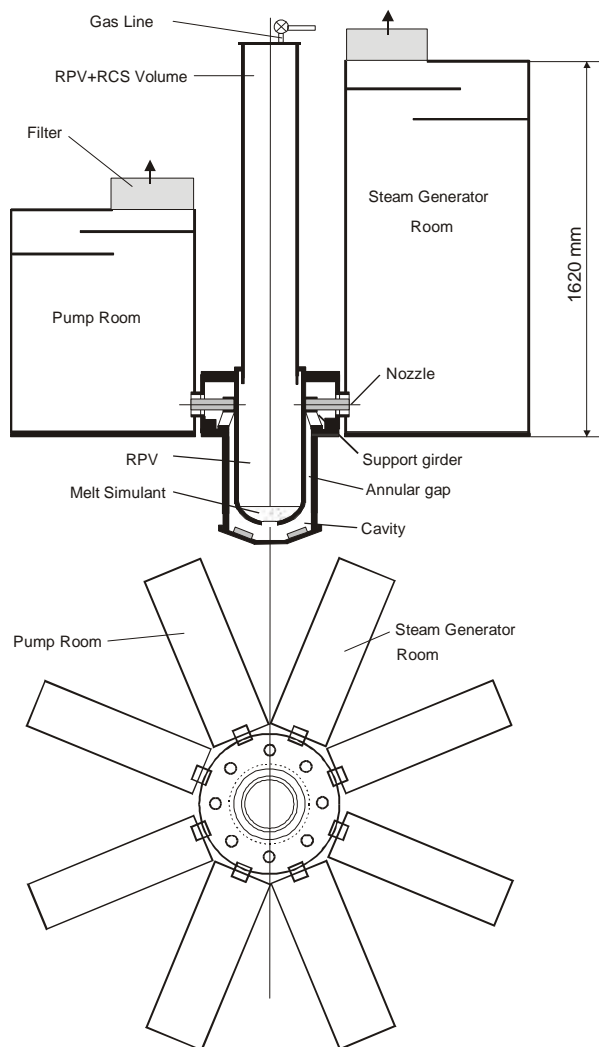


**Table 1** Main dimensions of the experiment

Geometric Parameters	
Pressure vessel volume, RPV + RCS (m <sup>3</sup> )	0.0879
RPV vessel OD (m)	0.2985
RPV lower head ID (curvature diameter) (m)	0.3000
RPV lower head volume (m <sup>3</sup> )	0.0036
Length from lower head base to cavity floor (m)	0.0620
Length from lower head base to nozzle centerline (m)	0.4850
Effective annular gap below nozzles (m)	0.02175
Flow area of annular gap (m <sup>2</sup> )	0.02188
Flow area at support girder (m <sup>2</sup> )	0.01890
Cavity diameter below nozzles (m)	0.3420
Cavity height (m)	0.6120
Hot and cold leg OD (m)	0.0500
Hot and cold leg cutout diameter (m)	0.0860
Hot and cold leg area (m <sup>2</sup> )	0.00196
Hot and cold leg cutout area (m <sup>2</sup> )	0.00581
Total leg area (m <sup>2</sup> )	0.01570
Total cutout area (m <sup>2</sup> )	0.04647
Total bypass flow area (cutout - leg) (m <sup>2</sup> )	0.03077
Pump room volume (each) (m <sup>3</sup> )	0.1311
Steam generator room (each) (m <sup>3</sup> )	0.2985

**Fig.1** Scheme of the DISCO-C test facility

## The experimental apparatus

A schematic diagram of the test facility DISCO-C is shown in Fig.1. It consists of three major parts, i.e., the pressure vessel, the cavity and the subcompartments. The pressure vessel is a steel pipe with a model of the reactor pressure vessel at its lower end. The cavity is made of a plexiglass cylinder attached to a steel structure that also holds the pressure vessel and eight boxes, which model the four steam generator and the four pump rooms, respectively. In the present test series the only flow path out of the reactor pit is the free flow area around the 8 main coolant lines into the pump and steam generator rooms. These rooms are open to the atmosphere, only covered by filters for the extraction of fog or droplets. In table 1 the main dimensions of the experiment are listed. The model matches the EPR-geometry in a scale 1:18.

The failure modes investigated in the first series were central holes in the lower head. These holes were closed by a rupture disk, that had an opening diameter larger than the hole diameter. In the second series that is presented in this paper, three types of lateral breaches were investigated. The first type are round holes of 25 and 50 mm diameter on the side of the lower head (Fig. 2). The inclination of the axis of the holes is 45 degrees. Their center measured at the inside is 50 mm above the bottom of the calotte. So, the lower edges of the holes at the inside are 41.15 and 32.4 mm above the bottom of the calotte, respectively. The second type is a horizontal slot, that models a partial rip in the lower head, as it might occur with a side-peaked heat flux distribution. The flow cross section is equivalent to a 25 mm hole (Fig. 3). The slot is 12.5 mm wide (high, inclined 45 degrees), and 42.5 mm long with a 6.25 mm radius. The lower edge of the slot is 56.1 mm above the bottom of the calotte. These two types of openings were closed by round rupture disks as with the central holes.

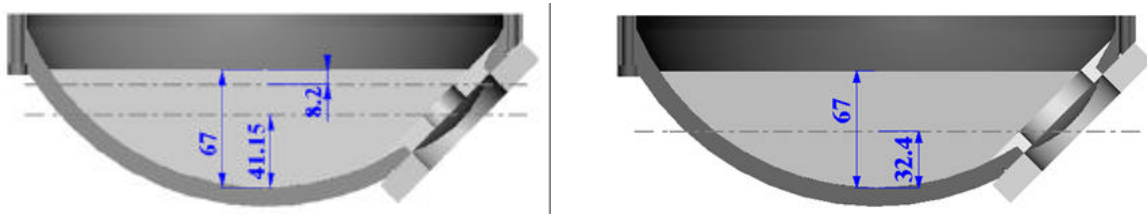


**Fig. 2** Geometry of lateral holes with 25 mm and 50 mm diameter



**Fig. 3** Geometry of lateral slot

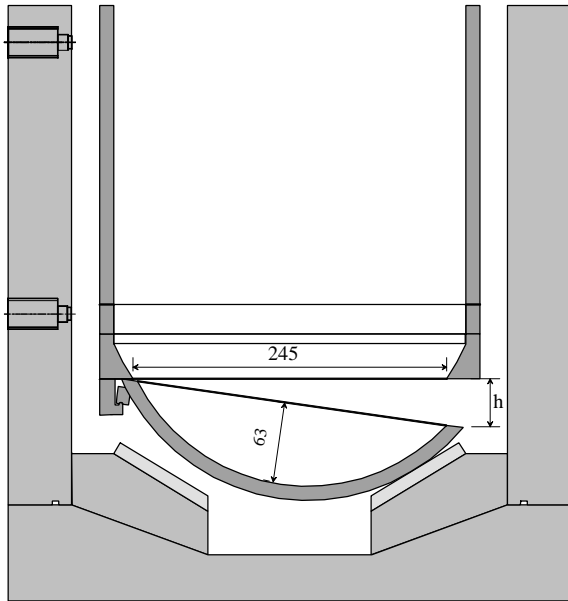


**Fig. 4** Unzipping and tilting of lower head

The third type models the horizontal rip propagating around the circumference of the lower head leaving only a small section attached (Fig.4), as it was observed in the lower head failure (LHF) experiments performed at SNL [8]. Here the calotte is a separate part that is held in position by a steel rod from below at its center. When it is released the lower head moves down on one side and is held by a hinge on the opposite side. It is stopped by crushing material on four pedestals. Two different heights of pedestals were used to obtain different flow cross sections. The maximum drop height was  $h = 56$  mm in one case, and  $h = 16$  mm in two other tests. The drop height at the side of the hinge was not zero but varied between 0.5 mm and 2 mm. The total flow cross section was  $220 \text{ cm}^2$  and  $70 \text{ cm}^2$ , respectively. For comparison, the cross section of a 100-mm-hole is  $79 \text{ cm}^2$  and for a 50-mm-hole it is  $20 \text{ cm}^2$ .

### The experimental procedure

The fluids employed in this test series were water or a bismuth alloy (MCP-58<sup>®</sup>, Bi-Pb-Sn-In-alloy, similar to Wood's metal) instead of corium, and nitrogen instead of steam (properties s. table 2). In the tests employing rupture disks, the pressure vessel is filled with gas to a pressure slightly lower than the failure pressure of the rupture disk. A small auxiliary pressure vessel (30 liter), filled to a somewhat higher pressure is connected to the main pressure vessel. By opening a valve electro-pneumatically in the line between the two vessels the pressure in the main vessel increases up to the failing pressure of the rupture disk and the blowdown starts. A break wire at the hole gives the signal for closing the valve again and for the time mark  $t = 0$ . The valve is closed at  $t = 70$  ms. In the tests with the declining lower head the experiment was started by breaking the bolts that held the rod in place by detonators.

**Table 2** Properties of the model fluids

Property		Nitrogen	Water	Bismut-alloy
Molecular weight	kg/kmol	28.013	18.015	165
Melting point	°C	-	0	58
Density $\rho$ at $10^5$ Pa	kg/m <sup>3</sup>	1.145	1000	9104
Dyn. Viscosity $\eta$ , 293 K	$10^{-3}$ Pa s	0.0178	1.002	$1.6^1$
Surface tension $\sigma$	$10^{-3}$ N/m	-	72	$350^1$

<sup>1</sup> estimated by taking the properties of the components from Liquid-Metals Handbook, NAVEXOS P-733, Atomic Energy Commission, Washington, D.C. 1952

Transient pressures were measured at 30 positions in the vessel, the cavity and the subcompartments. Piezo-resistive transducers were used, type Kistler, OEM RES12A, with ranges 2, 5, 10 and 20 bar absolute pressure. The sensors are compensated in the temperature range  $-20 \dots + 120$  °C. The sensors have a diameter of 12 mm and are mounted in the wall with the steel diaphragm almost flush with the wall. They have a high natural frequency, good linearity, low hysteresis ( $\pm 0.3\%$  FSO) and good reproducibility ( $< 0.2\%$ ).

Although the DISCO-C experiments are not intended to investigate thermal effects, temperatures must be measured because the gas temperature changes during the blowdown and the liquid metal must be heated above the melting temperature of 58°C. Three thermocouples in the pressure vessel and one in the lower cavity measure the gas and liquid temperature. The K-type thermocouples have a diameter of 0.36 mm. The time constant for gas temperature measurement is between 0.5 s and several seconds, depending on the heat transfer coefficient, with an estimate for our conditions of  $0.6 \text{ s} < \tau < 1.2 \text{ s}$ . Therefore all temperature signals for gas will be attenuated.

With the information of pressure and temperature in the pressure vessel and in the cavity, and the flow cross section of the annular space around the RPV, a mean gas velocity in the annulus,  $u_G$ , can be determined.

The mass fraction of the water or liquid metal in the compartments was determined by weighing the boxes before and after the test with a precision scale with an uncertainty of  $\pm 0.1$  gram. The water in the cavity was absorbed in dry cloth, that was weighed. The metal was solid after the test and could be weighed directly.

Two high speed film cameras (LOCAM II, 500 frames/second) are used to record the flow phenomena in the cavity; they are arranged in a view angle of 90 degree to each other. Additionally two CCD-video cameras are taking pictures from the cavity for a quick view. The liquid flow along the cooling pipes into the subcompartments is filmed by a CCD-video camera with high shutter speeds (50 frames /second).

The pressure and temperature data are acquired by a Data Translation Board DT2839 at a sampling rate of 2.5 kHz. 30 channels for pressure and 4 channels for temperature are currently used. Additionally, signals are recorded from the electro-pneumatic valve (open/closed) and the break wire as a time-zero and sync-signal.

## Results and discussion

In order to understand the differences between central holes and lateral breaches in the lower head we have to recapitulate the most important findings from the first experimental series. With central holes we can distinguish four stages in the blowdown process:

- 1., the single-phase liquid flow,
- 2., the blowthrough with two-phase flow,
- 3., single-phase choked flow, and
- 4., subsonic single-phase gas flow.

The duration of the individual phases depends on the hole size, the height of the liquid in the lower head, the pressure and the liquid density. The time of blowthrough can be expressed in terms of the height of the liquid at which the blowthrough occurs [7,9]. The time is short for large hole sizes  $d_h$  and high liquid velocities, i.e. high pressures and low liquid densities.

In the first stage, the single-phase liquid flow is driven by the static pressure in the vessel with the liquid velocity  $u_L = (2 \Delta p / \rho_L)^{1/2}$ . The liquid moves up the cavity walls by its inertia and can reach the subcompartments before any gas has left the vessel. During the second stage, the two phase flow, the liquid is accelerated by the gas, within the jet as a dispersed droplet flow and in the cavity by shear force along the liquid film. This stage is important in the reactor case, because the thermal and chemical interaction between steam and melt is high due to the large liquid surface area. Liquid is easily carried out of the pit during this stage. The third and fourth stage are characterized by high gas velocities in the reactor pit, and if the mass flow rate of the gas is high enough large fractions of the liquid can still be carried into the compartments. The results of the experiments with central holes concerning the dispersed fractions into the compartments,  $f_d$ , could be correlated by the Kutateladze number  $Ku = \rho_G u_G^2 / (\rho_L g \sigma)^{1/2}$ , with  $u_G$ , the maximum gas velocity in the annular space around the RPV, for all hole sizes, both driving gases, nitrogen and helium, and both liquids, water and Bi-alloy, with  $f_d = 0.4 \log_{10}(Ku) \leq 0.76$ .<sup>2</sup> Liquid fractions larger than 0.76 were not found in the compartments, but this is a specific feature of the geometry. Up to 25% of the liquid were captured in the space at the support girder.

**Table 3** Parameters and dispersed liquid fractions

Test	Liquid volume (10 <sup>-3</sup> m <sup>3</sup> )	Liquid	Issue	Hole Dia. (mm)	Flow cross section (cm <sup>2</sup> )	Burst pressure (MPa)	Liquid fraction found in				
							compartments $f_d$	Cavity bottom $f_B$	RPV support $f_s$	Cavity total $f_c = f_B + f_s$	RPV
D-20	1.8	water	central hole	25	5	1.140	0.553	0.024	0.423 <sup>§</sup>	0.447	0
D-05	3.4	water	central hole	50	20	1.200	0.759	0.012	0.229	0.241	0
M-01	3.1	metal	central hole	25	5	1.045	0.358	0.428	0.215	0.643	0
R-01	1.8	water	lateral slot	equiv.25	5	0.611	0.029*	0.423	0.185	0.608	0.363
R-02	1.8	water	lateral slot	equiv.25	5	1.101	0.250*	0.244	0.244	0.488	0.262
R-03	1.8	water	lateral hole	25	5	1.100	0.358*	0.294	0.238	0.531	0.111
R-06	1.8	water	lateral hole	25	5	1.610	0.469*	0.204	0.242	0.446	0.085
R-04	1.8	water	lateral hole	50	20	1.100	0.477*	0.266	0.209	0.475	0.048
R-05	1.8	metal	lateral hole	25	5	1.050	0.0005	0.657	0.006	0.663	0.336
D-08	3.4	water	central hole	100	78	0.613	0.717	0.052	0.231	0.283	0
K-01	2.1	water	unzipping	h=56	220 <sup>#</sup>	0.500	0.011*	0.851	0.043	0.894	0.095
K-02	2.1	water	unzipping	h=16	70	0.800	0.225*	0.320	0.270	0.588	0.187
K-03	2.0	metal	unzipping	h=16	70	1.100	0.008	0.455	0.124	0.579	0.413

\* most liquid was found in the compartments opposite of the slot or hole

# maximum possible flow cross section (D = 245 mm) : 471 cm<sup>2</sup>

§ closed holes at the support girder prevented a back flow into reactor pit

<sup>2</sup> The Kutateladze number represents the conditions to levitate droplets against gravity; some authors use  $Ku^2$  for the same expression. Index G stands for gas and L for liquid.

### Lateral holes

The results of the tests series with lateral failures are listed in table 3 together with some of the results of tests with central holes, that are suited best for comparison. When the breaches are not at the center but on the side of the lower head, only part of the liquid blocks the flow cross section, depending on the liquid inventory and the vertical position of the upper and lower edges of the holes. In all tests with lateral holes the liquid volume was 1800 cm<sup>3</sup>, the liquid level being 67 mm above the bottom of the calotte and near the upper edge of the holes. With the 25-mm-hole the level was 8.2 mm above the upper edge and with the 50-mm-hole it was 0.6 mm below the edge (s. Fig. 2).

From the vessel pressure curves (Fig.5) and the gas velocity curves (Fig.6) we can deduce that the blowthrough occurs very early (approximately at  $t \leq 0.1$  s). In Fig.5 we see that the theoretical pressure curve for single phase gas flow is steeper than the measured one for test R04 at early times. Therefore we can assume that the flow through the hole is two-phase even at times later than  $t = 0.1$  s, however, with a lower liquid fraction than in test D05 with a central hole, where we have an almost linear pressure decrease up to  $t = 0.3$  s.

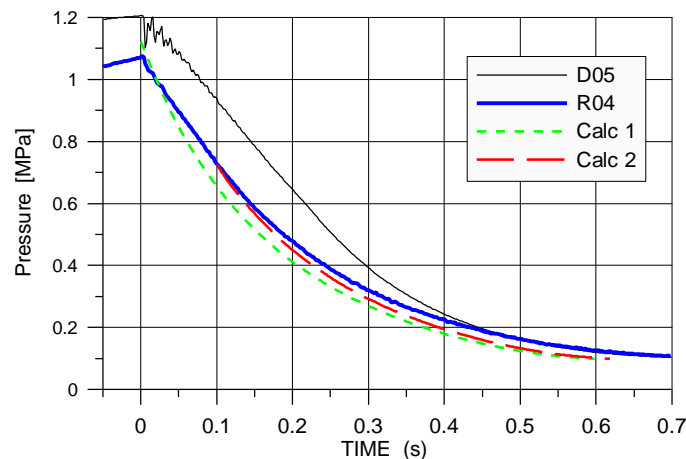


**Fig. 5** Comparison of blowdown pressure of experiments with central hole (D05) and lateral hole (R04), and with single-phase gas blowdown calculated for isentropic flow [9]

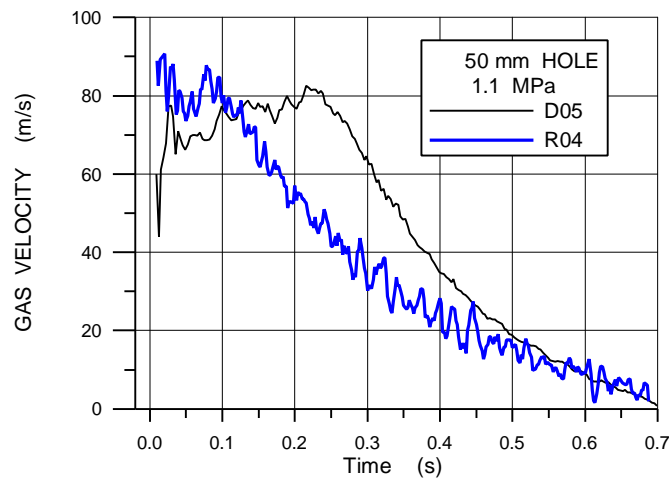


**Fig.6** Bulk gas velocities of nitrogen in the annular space in the cavity for tests with 50 mm-holes and liquid water, comparison of different hole positions (D05 and R04)

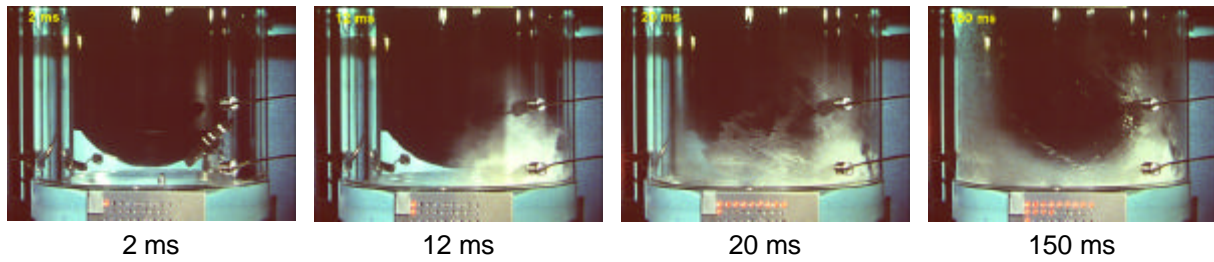


**Fig. 7** Flow in the reactor pit in test with lateral slot (test R01, typical for all slots and holes)

Fig.7 shows pictures of the flow in the cavity. The main direction of the flow is not vertical as with the central holes but in an angle of approximately 45 degree. Therefore, the velocities in the annular space, determined from the measured pressures with the vertical component only, deviate from the actual ones.

**Table 4** Lateral breaks data on post test liquid level in the lower head and reduced dispersed fraction  $f_d^*$  (pre-test level was 67 mm for the R-tests and 73 mm for K-tests)

Test	diameter or drop height [mm]	liquid	P [MPa]	lower edge	water level	Diff. [mm]	$f_{RPV}$	$f_d$	$f_d^*$
R-01	slot 25 equiv.	water	0.6	56	39	17	0.363	0.029	0.045
R-02	slot 25 equiv.	water	1.1	56	33	23	0.262	0.250	0.339
R-03	25	water	1.1	41	21	20	0.111	0.358	0.403
R-06	25	water	1.6	41	18	23	0.085	0.469	0.513
R-04	50	water	1.1	32	14	18	0.048	0.477	0.501
R-05	25	metal	1.1	41	39	3	0.336	0.0005	0.0008
K-01	57	water	0.5	-	-	15	0.095	0.011	0.012
K-02	16	water	0.8	-	-	25	0.187	0.225	0.277
K-03	16	metal	1.1	-	-	10	0.413	0.008	0.013

The ejected liquid was found mainly in the compartments opposite to the position of the hole. Not all of the liquid was ejected out of the RPV (s. Table 3). The main parameter determining the fraction that remains in the lower head is of course the vertical position of the lower edge of the hole. It is, however, interesting to see how much lower than this edge the water level is after the test. This is a measure for the magnitude of the entrainment. Table 4 lists the data for the lower edge, the liquid level and the difference between the two. Although there is less water left in the calotte in R04 with the larger hole than in R03 with the small hole, the entrainment was somewhat smaller in R04. There are two effects reducing the entrainment. With the large hole the blowdown time is shorter, and because the water level is already lower the surface area is smaller. The entrainment in test R05 is much smaller with the high density liquid metal than with water. The fractions ejected into the compartments are smaller than in the experiments with central holes (R03-D20 and R04-D05). (D05 was performed with a larger amount of liquid mass; for a total mass of  $1.8 \times 10^3 \text{ m}^3$ , we estimate a dispersed fraction of  $f_{RPV}=0.612$ , based on comparative measurements with other hole sizes.) Even if the dispersed fraction is determined in relation to the mass that was ejected out of the RPV, the difference is still in the order of 0.15 ( $f_d^*$  in table 4). In the tests D20 and D05 practically no liquid remained on the cavity bottom while in R03 and R04 approximately 30% of the ejected water was found there.

The test R05 can be compared with test M01. In test M01 with the central hole the metal mass fraction ejected into the compartments was 36%, and 21% was captured at the RPV support. With the lateral hole practically no metal was found in the compartments and at the RPV support.

### Slots

Two tests with a small horizontal slot were performed. The only difference between test R02 (slot) and R03 (round hole) is the shape and the vertical position of the opening in the lower head. The flow cross section of the slot is equivalent to a 25-mm-hole. The vessel pressure curves of the slot and the lateral hole tests are almost identical and therefore the gas velocities are the same also (Fig.8).

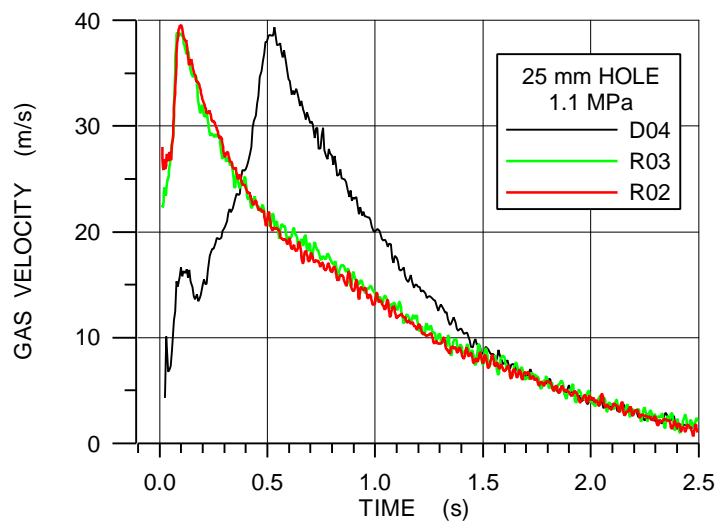


**Fig. 8.** Bulk gas velocities of nitrogen in the annular space in the cavity for 25 mm holes and liquid water, comparison of different hole position (D04 and R03), and different hole shape of lateral breaches (R03 and R02)

Due to the higher location of the lower edge of the slot more water remains in the calotte. The difference between post test water level and lower edge, however, is larger (23 versus 20 mm), and therefore the entrained amount of water. The reasons could be the larger surface area of the water pool in the calotte at this higher position, and the wider flow cross section of the slot versus a round hole. The dispersed liquid fraction is smaller with the slot. In relation to the total amount of water ejected out of the RPV, it is 34% for the slot and 40% for the hole (Table 4). The dispersed fraction at lower pressure (R01) is small with less than 5%. The correlation to the burst pressure is similar as that for small central holes, i.e. increasing  $f_d$  with increasing burst pressure (Fig.9). At lower pressure more water remains in the lower head, because the entrainment is smaller at lower gas velocity, lower density and shorter blowdown time.

### Unzipping of lower head

Corresponding to the large flow cross section with the high drop height of the calotte in test K01, the time for depressurization is extremely short with 0.08 seconds

(Fig.10). The other two tests, K02 and K03, with a drop height of 16 mm show a similar blowdown curve as tests D08 and D09, with the 100-mm-hole (Fig.10 and 11). As for the lateral holes and slots liquid remains in the lower head after the blowdown. The amount of liquid depends on the tilt angle of the calotte, that is higher for K01 than for the other two experiments, and on the entrainment. The entrainment is larger in test K02 compared to K01, because of the higher pressure and the larger surface area of the remaining water, and therefore the liquid level below the lowest edge of the tilted calotte is lower. With liquid metal (K03) the entrainment is much less due to its high density.

The liquid fraction dispersed out of the cavity is very small in test K01, with  $f_d = 0.011$ . With the central 100-mm-hole at an even lower pressure (D14,  $p = 0.35$  MPa) it was  $f_d = 0.580$ . The large break cross section does not lead to high dispersion rates, because the gas does not accelerate the liquid with the lateral break and the entrainment is small because of the extremely short blow down time. With a smaller drop height (smaller flow cross section) and a somewhat higher burst pressure of 0.8 MPa in test K02 the reduced dispersed fraction is higher ( $f_d^* = 0.277$ ), but still less than half of that of central holes with similar cross section (D08,  $f_d = 0.717$ ). Because the entrainment process plays the major role in the case of lateral breaches, the dispersed fraction with metal is very small (K03), even at the higher pressure of 1.1 MPa.

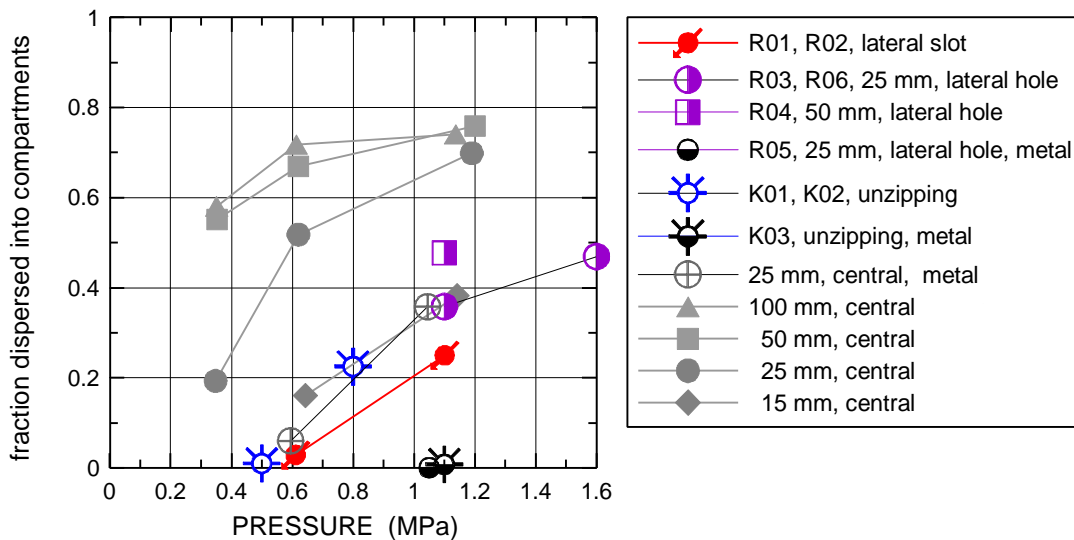


**Fig. 9** Dispersed fractions for special tests with lateral breaches and changes in cavity geometry in comparison with results from tests with central holes and water.

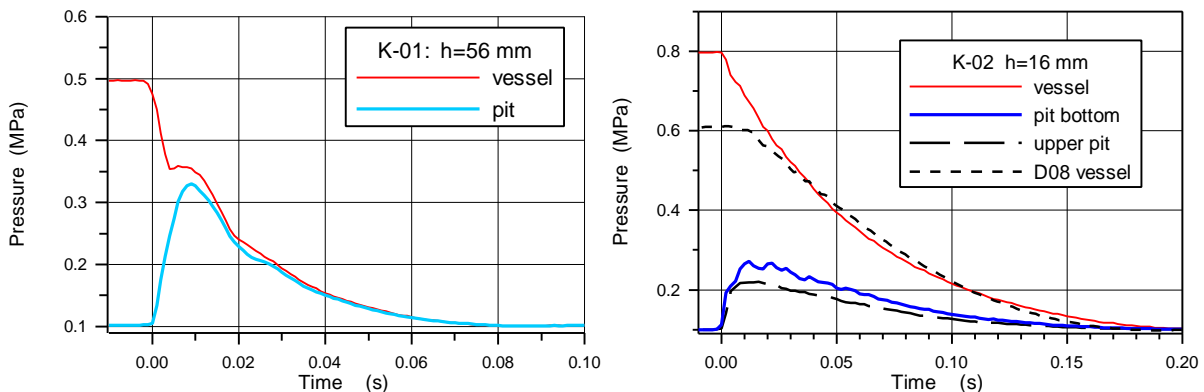


**Fig.10** Pressure in the pressure vessel and the reactor pit in tests with tilting of the lower head

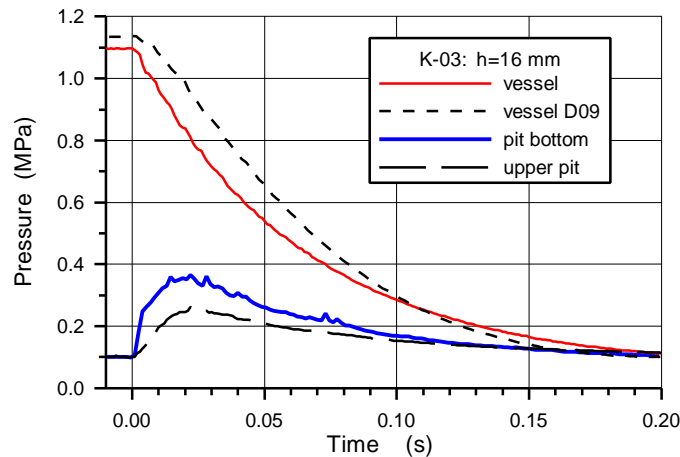


**Fig.11** Pressure in the pressure vessel and the reactor pit in tests K03 and D09

## Discussion and conclusion

Melt dispersion experiments with lateral failure in the bottom head were carried out in a 1:18 scaled annular cavity design under low pressure conditions. Water and a bi-mut-alloy were used as melt simulant material and nitrogen as driving gas. With holes at the base of the bottom head the most important parameters governing the dispersion of melt are the hole size and the burst pressure. Practically no liquid remains in the RPV. With lateral breaches the liquid height in the lower head relative to the upper and lower edge of the breach is an additional parameter for the dispersion process. In most cases not all the liquid is discharged out of the RPV. If the initial liquid level is above the upper edge the blowdown starts with the single-phase liquid discharge, driven by the pressure difference between vessel and cavity, as for central holes. However, the gas blowthrough occurs earlier. In the subsequent stage the liquid is carried out of the lower head by entrainment. The gas velocity at the breach may be high but the velocity above the liquid surface inside the vessel is much lower. It starts with zero at the opposite side of the breach and increases to the exit velocity. Besides the gas velocity, the density ratio of gas and liquid, the surface area of the liquid pool, and the duration of the blowdown govern the entrainment process. Therefore, the entrained liquid fraction can be higher with a small breach than with a large one, because the blowdown time is longer but the maximum velocity may be the same. The entrainment mechanism in such a case is not well understood and it is difficult to apply these results to the reactor case, since up to now, our experiments are the only ones with lateral breaches, and no other scale has been tested. Nevertheless, we can draw some important conclusions from our results.

Shifting the break from the central position towards the side of the lower head leads to a smaller dispersion of liquid, even if the dispersed fraction is related only to the liquid mass that has been ejected out of the RPV. The main effect is probably the circumferential component of the velocity in the cavity. Also, the velocity of the entrained droplets may be lower, because of the short entrainment length within the lower head.

For lateral breaches, a larger breach size does not necessarily lead to a larger dispersed melt fraction, because the entrainment process inside the lower vessel head plays a major role for the ejection of the liquid mass out of the RPV.

For burst pressures of 1.1 MPa or smaller the maximum dispersed fractions for lateral breaches were 48% with water and less than 1% with liquid metal. Additional experiments with liquid metal at higher burst pressures are necessary to find out if higher dispersion rates are possible. To establish a correlation for the dispersed melt fraction with lateral breaches more tests are needed with the extra parameters of the vertical position of the break and the height of the liquid level.

The application of the new results to the reactor scale is more difficult than in the case of central holes. Investigations of similarity for the process of entrainment within the lower head have not been undertaken yet. The other tools for extrapolation to the reactor case are the codes. Zero-dimensional codes need correlations for the lateral breaches that are not available due to the limited data basis. CFD-codes have not been applied yet in three dimensions, but it is planned to do so. As for the time being, we can make the cautious statement, that taking the known similarity correlations, the results from the liquid metal tests represent the lower bound for the dispersed melt fractions, however, they are probably closer to the expected values than the results from the water tests, that represent the upper bound. So, significantly less dispersion of melt can be expected for lateral breaches at pressures below 1.1 MPa, probably less than 10%. If higher dispersion occurs, maybe due to higher pressure at failure, simple devices to mitigate the dispersion out of the cavity may be feasible. For the investigation of thermal and chemical effects experiments with alumina-iron melt and steam will be performed in a similar geometry.

**Acknowledgement:** This work was partially supported by the European Commission under the contract No. FIKS-CT-1999-00003 (ECOSTAR, 5th EC-Framework Programme)

## References

1. Nucl. Eng. Des., 164, 1996 (Topical Issue on DCH).
2. Bertodano, M. L. de, A. Becker, A. Sharon, R. Schnider, 1996. DCH Dispersal and entrainment experiment in a scaled annular cavity, Nucl. Eng. Des., 164, 271-285.
3. Blanchat, T.K., M. Pilch, and M.D. Allen, 1997. Experiments to Investigate Direct Containment Heating Phenomena with Scaled Models of the Calvert Cliffs Nuclear Power Plant, NUREG/CR-6469, SAND96-2289, Sandia National Laboratories, Albuquerque, N.M.
4. Blanchat, T.K., M.M. Pilch, R.Y. Lee, L. Meyer, and M. Petit, 1999. Direct Containment Heating Experiments at Lower Reactor Coolant System Pressure in the Surtsey Test Facility, NUREG/CR-5746, SAND99-1634, Sandia National Laboratories, Albuquerque, N.M.
5. Kim, S.B, R.J. Park, H.D. Kim, Chevall and M.Petit, Reactor Cavity Debris Dispersal Experiment with Simulant at Intermediate System Pressure, Proc. Seminar on Containment of Nuclear Reactors, Postconference to the 15th SMiRT, Seoul, Korea, August 23-24, 1999.
6. Meyer, L., G. Jacobs, D. Wilhelm, M. Gargallo, T. K. Blanchat, 1999. Experiments on Corium Dispersion after Lower Head Failure at Moderate Pressure, Post Conf. Seminar on Containment of Nuclear Reactors, Seoul, Korea, August 23-24.
7. L. Meyer, Experiments to Investigate the Low Pressure Corium Dispersion in EPR Geometry, Proc. OECD Workshop on Ex-Vessel Debris Coolability, Karlsruhe, Germany, 15-18 November 1999, Ed. H. Alsmeyer, Forschungszentrum Karlsruhe, FZKA 6475, 2000.
8. Chu, T.Y., M. Pilch, J.H. Bentz and A.Behbahani, Experimental Investigation of Creep Behavior of Reactor Vessel Lower Head, OECD/CSNI Workshop on In-Vessel Core Debris Retention and Coolability, Garching, Germany, 3-6 March, 1998.
9. Meyer, L. et al., Low Pressure Corium Dispersion Experiments in the DISCO-C Tests Facility with Cold Simulant Fluids, FZK-Report 6591, Forschungszentrum Karlsruhe, to be published in 2001.